On-the-Fly Guidance Training for Medical Image Registration

Yicheng Chen * Tongji University Shanghai, China

Shengxiang Ji *
Huazhong University of Science and Technology
Wuhan, China

2053186@tongji.edu.cn

u202015362@hust.edu.cn

Yuelin Xin * University of Leeds Leeds, UK

Kun Han University of California, Irvine Irvine, CA, USA Xiaohui Xie † University of California, Irvine Irvine, CA, USA

sc20yx2@leeds.ac.uk

khan7@uci.edu

xhx@ics.uci.edu

Abstract

This research explores a novel approach in the realm of learning-based image registration, addressing the limitations inherent in weakly-supervised and unsupervised methods. Weakly-supervised techniques depend heavily on scarce labeled data, while unsupervised strategies rely on indirect measures of accuracy through image similarity. Notably, traditional supervised learning is not utilized due to the lack of precise deformation ground-truth in medical imaging. Our study introduces a unique training framework with On-the-Fly Guidance (OFG) to enhance existing models. This framework, during training, generates pseudoground truth a few steps ahead by refining the current deformation prediction with our custom optimizer. This pseudoground truth then serves to directly supervise the model in a supervised learning context. The process involves optimizing the predicted deformation with a limited number of steps, ensuring training efficiency and setting achievable goals for each training phase. OFG notably boosts the precision of existing image registration techniques while maintaining the speed of learning-based methods. We assessed our approach using various pseudo-ground truth generation strategies, including predictions and optimized outputs from established registration models. Our experiments spanned three benchmark datasets and three cutting-edge models, with OFG demonstrating significant and consistent enhancements, surpassing previous state-of-the-arts in the field. OFG offers an easily integrable plug-and-play solution to enhance the training effectiveness of learning-based image registration models. Code at https://github. com/miraclefactory/on-the-fly-quidance.

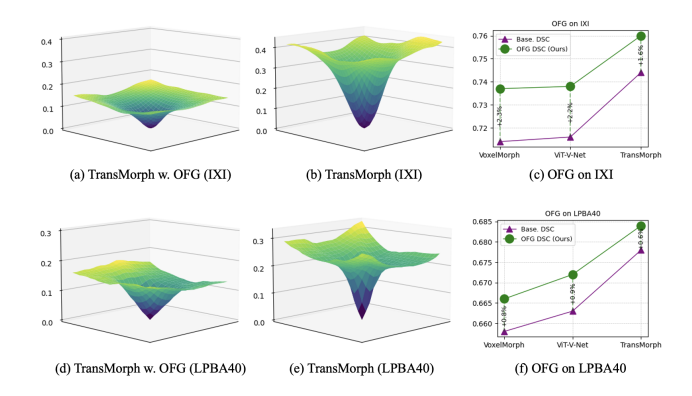


Figure 1. Loss landscape comparison between TransMorph with OFG and TransMorph without OFG on 2 datasets, (a)-(b), (d)-(e). The vertical axis represents the loss value, and the horizontal axes represent two principle directions in the parameter space. The landscapes illustrate the effect of OFG on the smoothness and convexity of the optimization surface. OFG in (a) and (d) produce much flatter loss landscapes, indicating improved trainability and better training outcomes, clearly shown in (c) and (f).

1. Introduction

Medical image registration plays a crucial role in various aspects of medical image analysis and finds numerous applications in modern medicine. Essentially, it involves the challenge of determining transformations, represented as a deformation field, to align two medical images (such as volumetric MRIs) in a manner that maximizes their visual similarity. Two primary approaches are commonly employed to tackle this challenge: optimization-based methods and learning-based methods. Traditionally, optimization-based methods like [4, 6, 42], iteratively enhance the deformation field by incorporating mathematical constraints. More re-

^{*}Equal contribution

[†]Corresponding author

cently, as learning-based methods, like those presented in [12, 13], have gained prominence, the field of image registration has swiftly embraced these techniques, which directly predict deformation fields from pairs of fixed and moving images.

Nevertheless, learning-based methods encounter a significant challenge. The two prevailing training approaches for deep learning registration models — namely weakly-supervised and unsupervised learning — each come with distinct advantages and drawbacks. Weakly-supervised learning, leveraging segmentation labels, typically produces superior registration outcomes [8], but the process of labeling datasets can be resource-intensive. In contrast, unsupervised learning eliminates the need for labeled data but strives to derive an accurate deformation field by comparing image similarities in the absence of pseudo-ground truth. Naturally, a pivotal question emerges: *Can we discover a training framework that avoids manually labeled ground truth while harnessing the advantages of direct supervision?*

In this paper, we introduce a unified framework with on-the-fly guidance (OFG) to incorporate supervised learning and enhance the performance of learning-based image registration methods. OFG employs instance-specific optimization to dynamically generate pseudo-ground truth during the training steps, using these optimized results to supervise image registration models. Our training framework adopts a novel hybrid approach that integrates direct prediction with iterative refinement, specifically tailored for the training phase. The process unfolds in two distinct but interconnected stages. In the prediction stage, the model being trained predicts a deformation field ϕ_{pre} during the forward pass. Subsequently, in the optimization stage, ϕ_{pre} is input to the optimizer module, which iteratively refines it, yielding an optimized deformation field ϕ_{ont} . Importantly, this optimized deformation field serves as a pseudo-label for training. The model is supervised through direct supervision between the optimized field and the initially predicted field: $MSE(\phi_{pre}, \phi_{opt})$, guiding the model's training alongside other regularization and loss functions.

Pseudo-supervision is facilitated through proposed onthe-fly guidance, a critical training technique that offers incremental supervision, guiding the model progressively toward convergence. Instead of providing the model with the ultimately optimized solution, we optimize the currently predicted deformation over limited (10) steps to derive a pseudo-ground truth as direct supervision, without adding too much overhead to the existing training paradigm. Importantly, by supplying incremental guidance alongside the training process, OFG mitigates the model's vulnerability to local minima, resulting in enhanced training outcomes. The integration of image registration models with on-the-fly guidance enables a more nuanced and self-improving training regimen. We also compared OFG with other pseudosupervision approaches, such as self-training, which utilizes the prediction or optimized prediction from pre-trained models. OFG consistently and significantly outperforms these methods, demonstrating the priority of our proposed framework.

The main contributions of our work are summarized as follows:

- We introduce OFG, a unified framework designed to enhance the performance of existing image registration methods. This framework incorporates both optimization and supervised learning into the training process while maintaining the efficiency of these methods during inference.
- The optimized pseudo-ground truth, generated iteratively during the training process, provides a more direct target for image registration models. Additionally, the on-thefly guidance establishes a self-improving relationship between the registration model and the optimizer module.
- Through comprehensive benchmarking across various models and datasets, our approach consistently outperforms baseline models, achieving superior performance compared to previous state-of-the-art methods.

2. Related Work

We will primarily be discussing these works in the context of medical image registration.

2.1. Weakly-Supervised & Unsupervised Training

Recent advancements have demonstrated that learningbased methods are gradually surpassing traditional optimization-based methods [2, 3, 10, 18, 19, 32, 49] in terms of performance and efficiency [14, 30, 39, 54]. Learning-based registration algorithms [8, 15, 22, 35– 37, 40, 41, 43–45, 48, 51] optimize the energy function in Eq. (5) for training dataset, aiming to acquire a global representation of the images being registered. While traditional supervised approaches [48, 51] rely on ground-trurh deformation fields typically generated through traditional registration methods, there has been a surge in unsupervised methods [8, 12, 13, 16, 43, 52]. A key innovation in this domain is the spatial transformer network (STN) [25]. For instance, VoxelMorph [8] utilizes a U-Net architecture to predict the deformation field and can utilize segmentation labels. Bob D. de Vos et al. [16] introduces a coarse-to-fine strategy in medical image registration. ViT-V-Net [12] integrates a Vision Transformer [17] block into the bottleneck of a U-Net architecture [24]. Lastly, TransMorph [13] combines a Swin Transformer [31] as the encoder with a ConvNet as the decoder. Although most of these methods can leverage auxiliary segmentation information for improved accuracy[8], such labels typically require costly manual annotations.

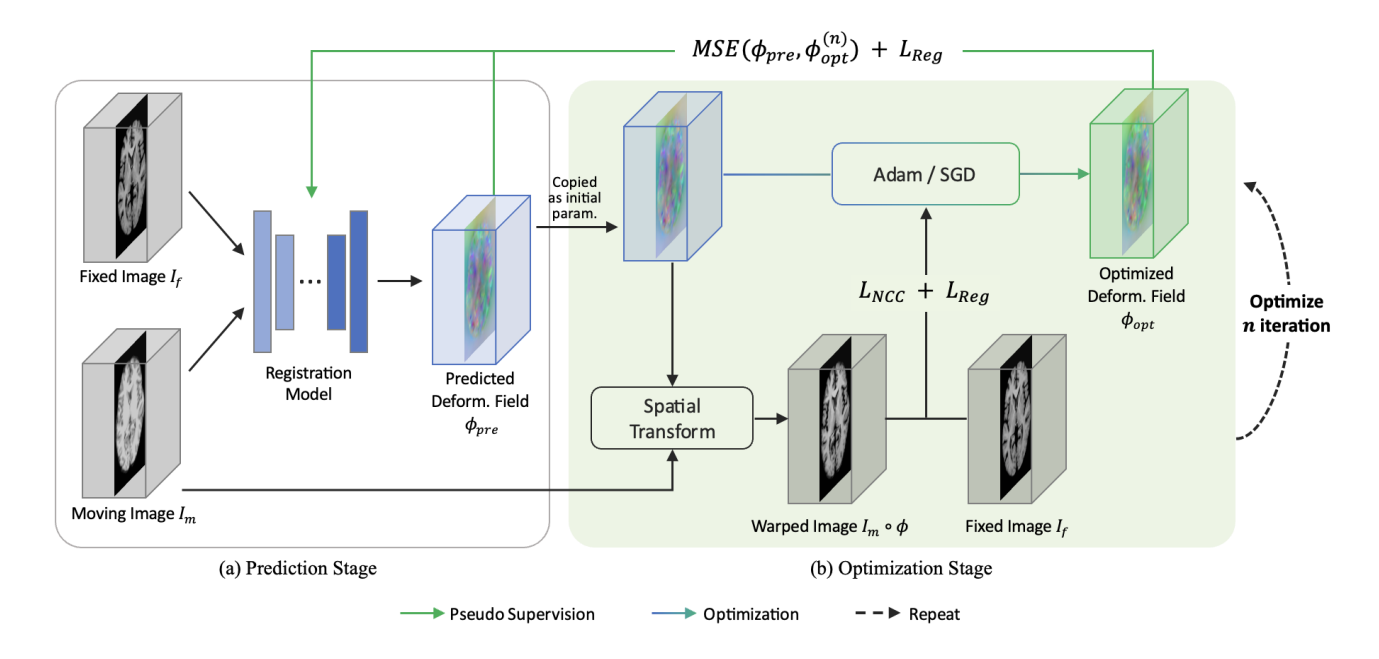


Figure 2. The overall structure of the proposed framework. The framework is divided into two parts, the prediction stage (any registration model that can predict a deformation field), and the optimization stage. The framework uses the idea of on-the-fly guidance to integrate the optimizer into the training process. The optimizer will iteratively refine the deformation field predicted by the registration model, the derived optimized deformation field will then be used as pseudo ground truth to train the registration model.

2.2. Unsupervised Training with Optimization

Recent advancements in computer vision have seen the growing application of on-the-fly guidance frameworks, leveraging instance-specific optimization for various tasks. These include image registration [9, 38], segmentation [53], and human pose estimation [28]. In the realm of image registration, the study in [47] effectively captures large deformations through discretized displacements coupled with a convex optimization process. [9] introduces a self-supervised learning paradigm based on cyclical self-training, utilizing a feature-based differentiable optimizer. Meanwhile, [38] presents Neural Instance Optimization (NIO) to correct biases in the deformation field caused by distribution shifts in deep-learning methods, while also incorporating prior knowledge from the training domain.

Most relevant to our work is [9], which leverages a differentiable convex discrete optimisation approach [46] to predict refined deformation fields. This self-training approach utilizes pseudo labels to guide the training across different stages. However, a notable distinction lies in their optimizer, which is used to find a transformation with a input of the fusion of semantic and hand-crafted image features, leading to non-learnable deformation field generation. Such an approach is in contrast with the utilization of existing unsupervised methods [8, 12, 13]. Additionally, unlike our OFG strategy, the method presented in [9] employs pseudo labels between training stages rather than within a single

training iteration. This could potentially lead to higher convergence complexity, a challenge in updating the base network for desired outcomes.

3. Method

In this work, we present a two-stage training framework with the proposed on-the-fly guidance (OFG) using pseudoground truth, which embeds optimization and supervised learning in the training of image registration models. In the following sections, we will discuss the overall structure of OFG, the key ideas and insights behind our design, alongside the implementation details of our method. In the following sections, I_m and I_f denote the moving image and fixed image respectively, ϕ_{pre} and ϕ_{opt} denotes the predicted deformation field and the optimized deformation field.

3.1. Overall Structure

Fig. 2 presents the overall structure of the proposed twostage training framework.

Prediction Stage. This stage consists of a learning-based registration model. The registration model takes a fixed image I_f and a moving image I_m and predicts a dense deformation field ϕ for each image pair I_f and I_m , i.e.,

$$F_{\theta}(I_f, I_m) = \phi \tag{1}$$

where θ denotes the parameters of the registration network.

Since OFG is a unified training framework, the prediction stage can utilize the desired existing learning-based registration model that predicts a deformation field. In our experiments, we used several popular models, such as VoxelMorph [8], ViT-V-Net [12] and TransMorph [13] in the prediction stage.

Optimization Stage. The optimization stage utilizes the proposed optimizer to iteratively refine the deformation field ϕ_{pre} predicted from the current training step by several steps (10 in our default setting). Subsequently, the optimized deformation field ϕ_{opt} is used as the pseudo-ground truth to provide supervision for the current predicted deformation during the training, forming a feedback loop between the prediction model and the optimizer module.

3.2. Training with Pseudo Ground Truth

Diverging from conventional image registration methods that rely on indirect supervision due to the absence of ground truth deformation fields, our approach involves leveraging pseudo labels generated by the optimizer mentioned earlier, providing structured and direct guidance. Within our study, we explore multiple methods for generating pseudo-ground truth. The most straightforward approach involves using the predictions from the pre-trained model as pseudo labels, akin to previous knowledge distillation methods. However, this method has a limitation: the pre-trained model's performance sets an upper bound for the current model. Another option is to iteratively optimize the predicted deformation from the pre-trained models until convergence, using the ultimately optimized deformation field as the pseudo-ground truth. This has the potential for improved performance but faces challenges due to the unique nature of image registration. Unlike tasks such as image segmentation, where predicted results align closely with the input image, the registration model must compare features from both input images to generate a reasonable deformation field. We argue that directly employing the ultimately optimized deformation offers minimal improvement, as evidenced by the substantial discrepancy between predicted deformation and pseudo ground truth during training, as demonstrated in the experiment section. Consequently, we introduce a novel method for pseudoground truth generation, incorporating on-the-fly guidance, which will be detailed in the next section.

3.3. On-the-Fly Guidance

Rather than relying on a fixed pseudo ground truth derived from either the pre-trained model's prediction or an ultimately optimized deformation, our approach introduces onthe-fly guidance. This dynamic supervision evolves alongside the training process to address discrepancies between pseudo labels and current predictions. In each training step, we utilize the current predicted deformation field as input



Figure 3. An illustration of the self-improving on-the-fly guidance, showing a tight integration between the prediction stage and the optimization stage.

for an online optimizer, subjecting it to optimization for a limited number of steps (typically 10 in the default setting). This approach offers two advantages: firstly, the minimal number of optimizations incurs acceptable overhead during training, and secondly, the optimized deformation serves as an attainable goal for the ongoing training step, providing more direct guidance for optimizing model parameters. In essence, on-the-fly guidance delivers incremental supervision, offering step-by-step and targeted guidance for the model. Moreover, this strategy possesses inherent selfimprovement characteristics. A well-estimated deformation field from the registration model provides a superior initialization for the optimizer, leading to a better-optimized deformation field. This improved deformation field, in turn, offers enhanced supervision back to the model, establishing a positive feedback loop between prediction and optimization. (Fig. 3).

3.4. Online Optimizer

An efficient and effective optimizer is the key to on-the-fly guidance. We explored three different optimization strategies: network-based optimization, downsampled optimization, and the proposed optimizer as shown in Fig. 2 (b). The proposed design achieves the best performance (see Tab. 3 and Tab. 4) due to its instance-specific optimization strategy and high degree of freedom for parameter updating. The detail of the other two optimizers would be introduced in Sec. 4.6.

The proposed optimizer is simple yet powerful, taking in the deformation field generated by the prediction model as its initial parameters and optimize it as the pseudo labels. Internally, it contains a Spatial Transformer Network (STN) [25], which introduces no additional parameter. Consequently, the only updatable parameters in the optimizer is the deformation field. During an optimization iteration, the current deformation field is applied to the moving image through the Spatial Transformer, yielding a warped image. Using the warped and the fixed image, an energy function will evaluate the discrepancy between the warped moving

image and the target image, and also the distortion of the deformation field. This discrepancy is backpropagated using methods like Adam [27] or Stochastic Gradient Descent (SGD), this essentially updates the deformation field, i.e.,

$$\phi_{opt}^{(n+1)} = \phi_{opt}^{(n)} - \eta \nabla E_{opt} \tag{2}$$

where n denotes the iteration step, η is the learning rate, and ∇E_{opt} represents the gradient of the optimization energy function, the detail of its implementation will be discussed later.

It is important to note that the optimization stage only serves its propose as the provider of supervision during training. The optimizer will not be used in inference time.

3.5. Implementation Detail

Overall Loss Function. The training of the registration model utilizes a composite loss function that combines the principles of supervision by pseudo-ground truth with regularization. The model learns by minimizing the discrepancy between the predicted deformation field ϕ_{pre} , and the optimized deformation field ϕ_{opt} , which is quantified using MSE. Simultaneously, a regularization term L_{reg} is incorporated to encourage a smooth deformation field. The overall loss implementation is as follows:

$$L_{all} = \frac{1}{n} \sum (\phi_{pre} - \phi_{opt})^2 + \lambda L_{reg}$$
 (3)

In this formula, L_{all} is the overall loss, where the first term is the MSE-based supervision and the second term represents the regularization loss, with λ acting as the regularization weight. For our model, λ is empirically set to 0.02 to ensure an optimal balance between fidelity of the deformation fields and the regularization constraint. The regularization loss is implemented as follows:

$$L_{reg}(\phi) = \sum_{p \in \Omega} ||\nabla \phi(p)||^2 \tag{4}$$

Optimizer Energy Function. The energy function to be minimized in the optimizer module consists of two terms: an image similarity loss term that computes the difference between the warped image $I_m \circ \phi$ and fixed image I_f and a regularization loss term that imposes smoothness in ϕ :

$$E_{opt}(I_m, I_f, \phi) = LNCC(I_f, I_m \circ \phi) + L_{reg}(\phi) \quad (5)$$

where \circ represents the transformation function which warps I_m using ϕ . The regularization term we used is the same as Eq. (4) and the similarity metric we used is the local normalized cross-correlation (NCC) between warped image $I_m \circ \phi$ and fixed image I_f :

$$LNCC(I_f, I_m \circ \phi) =$$

$$\sum_{p \in \Omega} \frac{(\sum_{p_i} (f(p_i) - \hat{f}(p))([I_m \circ \phi](p_i) - [\hat{I}_m \circ \phi](p)))^2}{(\sum_{p_i} (f(p_i) - \hat{f}(p))^2)(\sum_{p_i} ([I_m \circ \phi](p_i) - [\hat{f}_m \circ \phi](p))^2)}$$
(6)

where $\hat{I}_f(p)$ and $\hat{I}_m(p)$ represent the mean voxel value within a local window of size n^3 centered at voxel p.

4. Experiments

4.1. Experiment Conditions

Dataset and Preprocessing. This study employs three public datasets: IXI [33], OASIS [34], and LPBA40 [50]. For all datasets, we conduct standard preprocessing procedures on structural brain MRI data using FreeSurfer [5], including skull stripping, resampling, and affine transformation. The volume dimension is $160 \times 192 \times 224$ for IXI and OASIS, and $160 \times 192 \times 160$ for LPBA40. Specifically, for IXI, we randomly selected 200 volumes for training and 20 volumes for validation. For OASIS, the selection includes 200 for training and 19 for validation. And for LPBA40, we used 30 volumes for training, 9 volumes for validation, and 1 volume as the atlas.

Evaluation Metrics. When assessing our approach, we employed two widely-used metrics. Firstly, we measured the volume overlap of anatomical segmentations, quantified using Dice score (DSC) [7, 8]. This metric offers insights into the accuracy of registration. Additionally, we evaluate the regularity of the deformation fields through the Jacobian matrix, denoted as $J_{\phi}(p) = \nabla \phi(p)$. Specifically, we calculate the count of non-background voxels for which $\% |J_{\phi}| < 0$, indicating regions where the deformation deviates from being diffeomorphic [1]. This helps assessing the deformation's spatial consistency.

Baseline Models. We validated our proposed framework based on various registration models that have previously demonstrated state-of-the-art performance in registration tasks. This comparison included two traditional methods and multiple learning-based methods:

- SyN [4]: For all datasets, mean squared error (MSE) was used as the objective function, along with three scales with 160, 80, 40 iterations, respectively.
- NiftyReg [11]: The sum of squared difference (SSD) was used as the objective function. We used three scales with 300 iterations each by default.
- VoxelMorph [8]: We adhered to the default parameters outlined for VoxelMorph-1 proposed in [8].
- ViT-V-Net [12]: We applied the default network hyperparameter settings suggested in [12].
- TransMorph [13]: We applied the default hyperparameter settings of TransMorph in [13].

Experiment Settings. All models were trained on NVIDIA RTX 4090 for 500 epochs using Adam [26], with an initial learning rate of 1e-4 and a batch size of 1. For the optimizer module in our architecture, we used an initial learning rate of 0.1, coupled with an optimization iteration count of 10 during training.

Datasets	Methods	Base. DSC ↑	$\mathbf{OFG}\mathbf{DSC}\uparrow$	Base. $\% J_{\phi} < 0 \downarrow$	OFG $\% \mathbf{J}_{\phi} < 0 \downarrow$	Infer. Time (s)
IXI [33]	SyN [4]	0.647	N/A	1.96e-6	N/A	277(CPU)
	NiftyReg [11]	0.585	N/A	0.029	N/A	22.4(CPU)
	VoxelMorph [8]	0.714	0.737 (+2.3%)	1.398	0.516 (-0.882)	0.061(GPU)
	ViT-V-Net [12]	0.716	0.738 (+2.2%)	1.543	0.545 (-0.998)	0.615(GPU)
	TransMorph [13]	0.744	0.760 (+1.6%)	1.433	0.794 (-0.639)	0.114(GPU)
OASIS [34]	SyN [4]	0.769	N/A	1.58e-4	N/A	258(CPU)
	NiftyReg [11]	0.762	N/A	0.011	N/A	25.0(CPU)
	VoxelMorph [8]	0.788	0.794 (+0.6%)	0.911	0.490 (-0.421)	0.061(GPU)
	ViT-V-Net [12]	0.794	0.809 (+1.5%)	0.887	0.487 (-0.400)	0.646(GPU)
	TransMorph [13]	0.818	0.818 (=)	0.765	0.517 (-0.248)	0.160(GPU)
LPBA40 [50]	SyN [4]	0.703	N/A	1.18e-4	N/A	172(CPU)
	NiftyReg [11]	0.691	N/A	1.13e-3	N/A	22.8(CPU)
	VoxelMorph [8]	0.658	0.666 (+0.8%)	0.288	0.023 (-0.205)	0.046(GPU)
	ViT-V-Net [12]	0.663	0.672 (+0.9%)	0.390	0.112 (-0.278)	0.446(GPU)
	TransMorph [13]	0.678	0.684 (+0.6%)	0.438	0.150 (-0.288)	0.327(GPU)

Table 1. Evaluation results for different methods on various datasets. The OFG architecture provides significant and substantial improvement on the unsupervised learning-based methods. These results validate OFG's effectiveness and generalizability without compromising on inference efficiency.

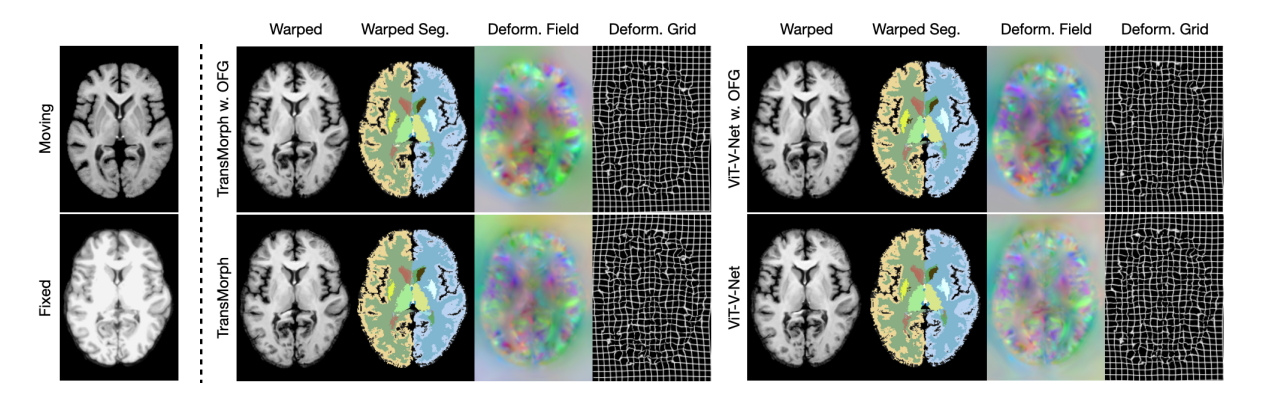


Figure 4. Visualization of registration results. This is an arbitrary demo extracted from the comparison results between baseline Trans-Morph, ViT-V-Net (row 2) and their respective model trained with OFG (row 1), demo from the IXI dataset [33]

4.2. Image Registration Results

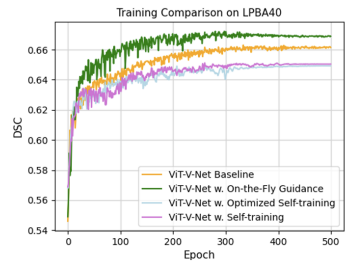
We conducted extensive experiments on the three datasets to showcase the effectiveness of our proposed framework. Moreover, to demonstrate the plug-and-play versatility of our approach, we implemented OFG on three learning-based registration networks: VoxelMorph [8], ViT-V-Net [12], and TransMorph [13].

OFG on IXI. OFG considerably increased DSC over the original learning-based models, as evidenced in Tab. 1. Notably, it outperformed the previous state-of-the-art, Trans-Morph [13], on the IXI dataset, achieving a +1.6% improvement in DSC and halving the percentage of non-diffeomorphic voxels ($|J_{\phi}| < 0$). This suggests OFG's

capability to not only elevate model performance but also to prevent the generation of over-sharpened deformation fields, which can be visually observed by comparing the actual registration results as shown in Fig. 4. Furthermore, OFG substantially improved other learning-based methods, with a +2.3% increase on DSC for VoxelMorph [8] and a +2.2% increase on DSC for ViT-V-Net [12], further validating the effectiveness and generalizability of our method.

OFG on LPBA40. LPBA40 [50] is another dataset we used to validate our method. Evaluation results are presented in Tab. 1. With only 40 volumes, learning-based models can easily overfit on this dataset. This can be partially observed in the convergence phase in Fig. 5. On a





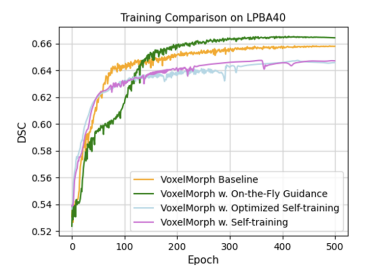


Figure 5. Visualization of training process vs. validation DSC for models on LPBA40. The self-training strategy utilizes deformation fields from a pre-trained network as pseudo-ground truth. In contrast, optimized self-training iteratively refines the deformation these fields, and then uses them as pseudo-ground truth. Our proposed method is highlighted for its superior outcomes. Notably, self-training schema underperforms, primarily due to complexities in convergence.

Converg. Loss	IXI [33]	OASIS [34]	LPBA40 [50]
VoxelMorph [8]	-0.222	-0.259	-0.183
ViT-V-Net [12]	-0.242	-0.266	-0.215
TransMorph [13]	-0.262	-0.283	-0.232

Table 2. Comparison between the 3 models' convergence losses on 3 datasets. Note that the loss function settings were the same. For TransMorph on OASIS, the convergence loss is clearly the lowest.

small dataset, the extra supervision provided by our method can be crucial due to the lack of training data. Supervision that introduces greater challenges into the training process can significantly enhance the model's learning, ultimately yielding superior results.

OFG on OASIS. OASIS [34] is another commonly used dataset in medical image registration. According to the results in Tab. 1, although all methods generally achieve higher DSC on this dataset, it's noteworthy that OFG yielded no noticeable improvement when applied to Trans-Morph on the OASIS dataset. It is likely due to the OASIS dataset presents a less stringent challenge for TransMorph. To validate this hypothesis, we employed image similarity loss as a metric; a lower loss score indicates a dataset is less challenging for a given method. This was substantiated by comparing the convergence loss of all models across various datasets, as detailed in Tab. 2. Among the diverse combinations of three models and three datasets assessed, TransMorph on the OASIS dataset demonstrated the lowest convergence loss, aligning with our hypothesis.

4.3. Training Guided by Pseudo Ground Truth

To evaluate the effectiveness of pseudo-ground truth described in Sec. 3.2, we compared the loss landscapes of TransMorph and TransMorph w. OFG on the IXI and LPBA40 datasets. Following the loss landscape visualization method described in [20, 23, 29], we chose a set of

	DSC	$% J_{\phi} < 0$	Optimize Time (s)
VoxelMorph-1	0.691	0.456	1.174
VoxelMorph-2	0.690	0.383	2.314
VoxelMorph-5	0.693	0.385	5.856
Ours	0.731	0.503	4.697

Table 3. Comparison between instance-specific optimizer (OFG) and network-based optimizer on IXI dataset[33]. The outcomes presented are derived from the initial 200 epochs.

pre-trained model's parameters θ^* as the center point in the graph, perturbed θ^* in two random directions and computed the average loss value on five samples from the validation set at each location. As shown in Fig. 1, the loss landscape of TransMorph w. OFG is substantially smoother and convex than that of other strategies. The flatter loss landscape of TransMorph w. OFG suggests better trainability, avoidance of local minima and better performance, which further demonstrates the advantage of our training method guided by pseudo label.

4.4. On-the-fly Guidance Strategy

To evaluate the effectiveness of our on-the-fly guidance strategy described in Sec. 3.3, we conducted a comparative analysis against an alternative approach. This approach utilized deformation fields, initially set by a well-trained network and subsequently refined iteratively by the OFG optimizer module, as pseudo-ground truth to guide training from scratch. The comparative results are detailed in Fig. 5 between the green line and the blue line. In contrast to our method, although initial learning occurs in the alternative strategy, it faces challenges in terms of convergence complexity. This comparison effectively demonstrates the superiority and efficiency of on-the-fly guidance strategy.

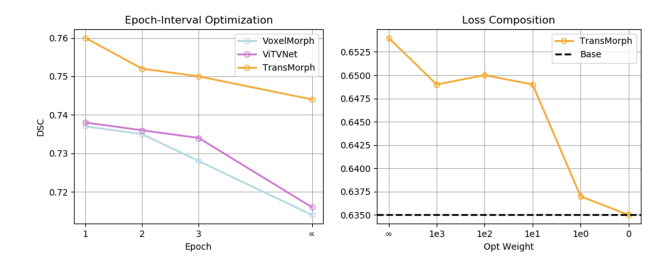


Figure 6. Ablation results. This evaluation investigates the impact of integrating unsupervised learning elements into our OFG system on IXI (left) and LPBA40 (right, 30 epochs). It reveals a notable decrease in performance with increased reliance on unsupervised methods, showing a 1.6% and 1.9% decline with Trans-Morph, respectively.

4.5. Instance-specific Optimization

To evaluate the efficacy of instance-specific optimization described in Sec. 3.4, we conducted a comparative study on a distinct optimizer design. An in-depth discussion of this optimizer, termed the Network-based optimizer, is provided in Sec. 4.6 Paragraph 1. VoxelMorph-n means repeating n epochs before providing pseudo-ground truth. The results, presented in Tab. 3, effectively demonstrate the superiority of instance-specific optimization within the OFG architecture. This optimizer module not only achieves the highest DSC, but also maintains a feasible optimization time.

4.6. Ablation Study

Optimizer Design. We designed a plug-and-play optimizer module to provide a more refined deformation field. Particularly, there are various approaches to optimizer design. Tab. 4 shows the performance of different optimizer schemes.

- Network-based Optimizer. Network-based optimizer aims to find a general transformation applicable to all instances. In this setup, for each epoch of the baseline network, the optimizer network initially updates its parameters iteratively for all images in the optimization set. Subsequently, the baseline network learns exclusively from the pseudo deformation fields generated by the optimizer network for each image pair in the training set.
- DownSample Optimizer. Optimizing the entire deformation field at once might be challenging [21]. By downsampling the deformation field, we can decrease the number of parameters being updated in every optimization iteration, which could lead to faster optimization routines. Additionally, downsampled deformation field can provide coarse-resolution information [35], which is crucial to the smoothness of the deformation field.

We observe that most optimizer designs demonstrate their effectiveness by surpassing the performance of none-

Optimizer Design	DSC	Time	VRAM Usage
None	0.635	N/A	12.07 GB
Network-based	0.642	13.604	14.35 GB
DownSample	0.610	0.097	12.44 GB
Ours	0.654	3.228	13.07 GB

Table 4. Ablation results of the OFG Optimizer on LPBA40 Dataset. This evaluation focuses over the initial 30 epochs.

optimizer version, except for the Downsample Optimizer. Among the evaluated strategies, the proposed OFG optimizer module achieves the highest Dice score while maintaining practical optimization time within a training iteration. The Downsample Optimizer, despite its acceleration of the optimization process, inadvertently compromises the quality of results. This occurs due to direct downsampling of the deformation field, resulting in a loss of finegranularity information and higher degrees of freedom, as discussed in Sec. 3.4. For the Network-based Optimizer, although it contributes to the optimization process, the efficacy is found to be suboptimal. Furthermore, the computational intensity and optimization time is impractical in our proposed architecture.

Importance of Pseudo-Ground Truth. We propose onthe-fly guidance strategy to circumvent the limitations inherent in the indirect learning mechanisms of unsupervised learning, as outlined in Sec. 3.2. To evaluate the effectiveness of this approach, as shown in Fig. 6, we contrast our method with two optimization strategy. Epoch-interval optimization involves the application of pseudo labels generated by the optimizer at specific epoch intervals, contrary to the continuous optimization present in our original OFG. Threshold-based optimization applies pseudo labels when a random value falls below a predetermined threshold. Moreover, we analyze Loss composition Eq. (7). In the aforementioned three experiments, the default configuration of the OFG fully incorporates supervision using pseudoground truth. As the parameters diverge from this original setting, there is a proportional increase in the reliance on unsupervised learning methods. Notably, in our analysis of the IXI dataset, we observe that our approach holds a great performance degradation with the increased incorporation of unsupervised learning elements within our approach. Furthermore, in our exploration of loss composition, we maintain the values of λ and β in Eq. (7) consistent with the original OFG settings, while introducing L_{sim} as an auxiliary component. This inclusion, however, results in diminished focus on the superior pseudo-ground truth, thus impairing performance.

$$L_{all} = \alpha L_{sim} + \lambda L_{req} + \beta L_{opt} \tag{7}$$

5. Conclusion

This work introduces On-the-Fly Guidance (OFG), a training framework that successfully unites learning-based methods with optimization techniques to enhance the training of learning-based registration models. Demonstrating significant improvements on benchmark datasets, outperforming existing methods, OFG has proven its effectiveness and generalizability. Future work may focus on optimizing the efficiency of the OFG training process with other optimizer designs to accelerate its adoption in practical applications.

References

- [1] John Ashburner. A fast diffeomorphic image registration algorithm. *NeuroImage*, page 95–113, 2007. 5
- [2] John Ashburner and Karl J. Friston. Voxel-based morphometry—the methods. *NeuroImage*, 2000. https://doi.org/10.1006/nimg.2000.0582. 2
- [3] Dalca AV, Bobu A, Rost NS, and Golland P. Patch-based discrete registration of clinical brain images. *Patch Based Tech Med Imaging* (2016), 2016.
- [4] B.B. Avants, C.L. Epstein, M. Grossman, and J.C. Gee. Symmetric diffeomorphic image registration with crosscorrelation: Evaluating automated labeling of elderly and neurodegenerative brain. *Medical Image Analysis*, 12(1):26– 41, 2008. Special Issue on The Third International Workshop on Biomedical Image Registration – WBIR 2006. 1, 5, 6
- [5] Fischl B. Freesurfer. Neuroimage, 2012. https://surfer.nmr.mgh.harvard.edu/. 5
- [6] Ruzena Bajcsy and Stane Kovačič. Multiresolution elastic matching. Computer Vision, Graphics, and Image Processing, 46(1):1–21, 1989. 1
- [7] Ruzena Bajcsy and Stane Kovačič. Multiresolution elastic matching. Computer Vision, Graphics, and Image Processing, page 1–21, 1989. 5
- [8] Guha Balakrishnan, Amy Zhao, Mert R. Sabuncu, John Guttag, and Adrian V. Dalca. VoxelMorph: A learning framework for deformable medical image registration. *IEEE Transactions on Medical Imaging*, 38(8):1788–1800, 2019. 2, 3, 4, 5, 6, 7
- [9] Alexander Bigalke, Lasse Hansen, Tony C. W. Mok, and Mattias P. Heinrich. Unsupervised 3d registration through optimization-guided cyclical self-training. In *Medical Image Computing and Computer Assisted Intervention – MICCAI* 2023, pages 677–687, Cham, 2023. Springer Nature Switzerland. 3
- [10] Ceritoglu C, Wang L, Selemon LD, Csernansky JG, Miller MI, and Ratnanather JT. Large deformation diffeomorphic metric mapping registration of reconstructed 3d histological section images and in vivo mr images. Front Hum Neurosci, 2010. 2
- [11] UK Centre for Medical Image Computing,
 University College London. Niftyreg, 2023.
 http://cmictig.cs.ucl.ac.uk/wiki/index.php/NiftyReg. 5,

- [12] Junyu Chen, Yufan He, Eric C. Frey, Ye Li, and Yong Du. Vit-v-net: Vision transformer for unsupervised volumetric medical image registration, 2021. 2, 3, 4, 5, 6, 7
- [13] Junyu Chen, Eric C. Frey, Yufan He, William P. Segars, Ye Li, and Yong Du. TransMorph: Transformer for unsupervised medical image registration. *Medical Image Analysis*, 82:102615, 2022. 2, 3, 4, 5, 6, 7
- [14] Qiguang Chen, Zhiwen Li, and Lok Ming Lui. A learning framework for diffeomorphic image registration based on quasi-conformal geometry. *CoRR*, abs/2110.10580, 2021.
- [15] Adrian V. Dalca, Guha Balakrishnan, John Guttag, and Mert R. Sabuncu. Unsupervised Learning for Fast Probabilistic Diffeomorphic Registration. arXiv e-prints, art. arXiv:1805.04605, 2018. 2
- [16] Bob D. de Vos, Floris F. Berendsen, Max A. Viergever, Hessam Sokooti, Marius Staring, and Ivana Išgum. A deep learning framework for unsupervised affine and deformable image registration. *Medical Image Analysis*, 52:128–143, 2019.
- [17] Alexey Dosovitskiy, Lucas Beyer, Alexander Kolesnikov, Dirk Weissenborn, Xiaohua Zhai, Thomas Unterthiner, Mostafa Dehghani, Matthias Minderer, Georg Heigold, Sylvain Gelly, Jakob Uszkoreit, and Neil Houlsby. An image is worth 16x16 words: Transformers for image recognition at scale, 2021. 2
- [18] Beg M. Faisal, Miller Michael I, Trouvé Alain, and Younes Laurent. Computing large deformation metric mappings via geodesic flows of diffeomorphisms. *International Journal of Computer Vision*, 2005.
- [19] Ben Glocker, Nikos Komodakis, Georgios Tziritas, Nassir Navab, and Nikos Paragios. Dense image registration through mrfs and efficient linear programming. *Medical Image Analysis*, 12(6):731–741, 2008. Special issue on information processing in medical imaging 2007.
- [20] Ian J. Goodfellow, Oriol Vinyals, and Andrew M. Saxe. Qualitatively characterizing neural network optimization problems, 2015. 7
- [21] Kun Han, Shanlin sun, Xiangyi Yan, Chenyu You, Hao Tang, Junayed Naushad, Haoyu Ma, Deying Kong, and Xiaohui Xie. Diffeomorphic Image Registration with Neural Velocity Field. arXiv e-prints, art. arXiv:2202.12498, 2022. 8
- [22] Jing Hu, Ziwei Luo, Xin Wang, Shanhui Sun, Youbing Yin, Kunlin Cao, Qi Song, Siwei Lyu, and Xi Wu. End-to-end multimodal image registration via reinforcement learning. *Medical Image Analysis*, 68:101878, 2021. 2
- [23] Daniel Jiwoong Im, Michael Tao, and Kristin Branson. An empirical analysis of the optimization of deep network loss surfaces, 2017. 7
- [24] Phillip Isola, Jun-Yan Zhu, Tinghui Zhou, and Alexei A. Efros. Image-to-image translation with conditional adversarial networks, 2018.
- [25] Max Jaderberg, Karen Simonyan, Andrew Zisserman, and Koray Kavukcuoglu. Spatial transformer networks, 2016. 2,
- [26] DiederikP. Kingma and Jimmy Ba. Adam: A method for stochastic optimization. arXiv: Learning, arXiv: Learning, 2014. 5
- [27] Diederik P. Kingma and Jimmy Ba. Adam: A method for stochastic optimization, 2017. 5

- [28] Nikos Kolotouros, Georgios Pavlakos, Michael J. Black, and Kostas Daniilidis. Learning to reconstruct 3D human pose and shape via model-fitting in the loop. In *Proceedings International Conference on Computer Vision (ICCV)*, pages 2252–2261. IEEE, 2019. ISSN: 2380-7504. 3
- [29] Hao Li, Zheng Xu, Gavin Taylor, Christoph Studer, and Tom Goldstein. Visualizing the loss landscape of neural nets, 2018. 7
- [30] Risheng Liu, Zi Li, Xin Fan, Chenying Zhao, Hao Huang, and Zhongxuan Luo. Learning deformable image registration from optimization: Perspective, modules, bilevel training and beyond. *IEEE Transactions on Pattern Analysis and Machine Intelligence*, 44(11):7688–7704, 2022. 2
- [31] Ze Liu, Yutong Lin, Yue Cao, Han Hu, Yixuan Wei, Zheng Zhang, Stephen Lin, and Baining Guo. Swin transformer: Hierarchical vision transformer using shifted windows, 2021. 2
- [32] Dirk Loeckx, Frederik Maes, Dirk Vandermeulen, and Paul Suetens. Nonrigid image registration using free-form deformations with a local rigidity constraint. In *Medical Image Computing and Computer-Assisted Intervention – MICCAI* 2004, pages 639–646, Berlin, Heidelberg, 2004. Springer Berlin Heidelberg. 2
- [33] Imperial Collage London. Information extraction from images, 2023. https://brain-development.org/ixi-dataset/. 5, 6,
- [34] Daniel S. Marcus, Tracy H. Wang, Jamie Parker, John G. Csernansky, John C. Morris, and Randy L. Buckner. Open Access Series of Imaging Studies (OASIS): Cross-sectional MRI Data in Young, Middle Aged, Nondemented, and Demented Older Adults. *Journal of Cognitive Neuroscience*, 19 (9):1498–1507, 2007. 5, 6, 7
- [35] Tony C. W. Mok and Albert C. S. Chung. Large deformation diffeomorphic image registration with laplacian pyramid networks, 2020. 2, 8
- [36] Tony C. W. Mok and Albert C. S. Chung. Fast symmetric diffeomorphic image registration with convolutional neural networks, 2021.
- [37] Tony C. W. Mok and Albert C. S. Chung. Affine medical image registration with coarse-to-fine vision transformer, 2022.
- [38] Tony C. W. Mok, Zi Li, Yingda Xia, Jiawen Yao, Ling Zhang, Jingren Zhou, and Le Lu. Deformable medical image registration under distribution shifts with neural instance optimization. In *Machine Learning in Medical Imaging*, pages 126–136, Cham, 2024. Springer Nature Switzerland. 3
- [39] Abdullah Nazib, Clinton Fookes, and Dimitri Perrin. A comparative analysis of registration tools: Traditional vs deep learning approach on high resolution tissue cleared data, 2018.
- [40] Marc-Michel Rohé, Manasi Datar, Tobias Heimann, Maxime Sermesant, and Xavier Pennec. Svf-net: Learning deformable image registration using shape matching. In *Medi*cal Image Computing and Computer Assisted Intervention -MICCAI 2017, pages 266–274, Cham, 2017. Springer International Publishing. 2

- [41] Ameneh Sheikhjafari, Michelle L. Noga, K. Punithakumar, and Nilanjan Ray. Unsupervised deformable image registration with fully connected generative neural network, 2018.
 2
- [42] Dinggang Shen and C. Davatzikos. Hammer: hierarchical attribute matching mechanism for elastic registration. *IEEE Transactions on Medical Imaging*, 21(11):1421–1439, 2002.
- [43] Zhengyang Shen, Xu Han, Zhenlin Xu, and Marc Niethammer. Networks for Joint Affine and Non-parametric Image Registration. arXiv e-prints, art. arXiv:1903.08811, 2019.
- [44] Zhengyang Shen, François-Xavier Vialard, and Marc Niethammer. Region-specific Diffeomorphic Metric Mapping. arXiv e-prints, art. arXiv:1906.00139, 2019.
- [45] Jiacheng Shi, Yuting He, Youyong Kong, Jean-Louis Coatrieux, Huazhong Shu, Guanyu Yang, and Shuo Li. XMorpher: Full Transformer for Deformable Medical Image Registration via Cross Attention. arXiv e-prints, art. arXiv:2206.07349, 2022. 2
- [46] Hanna Siebert and Mattias P. Heinrich. Learn to fuse input features for large-deformation registration with differentiable convex-discrete optimisation. In *Biomedical Image Registration*, pages 119–123, Cham, 2022. Springer International Publishing. 3
- [47] Hanna Siebert, Lasse Hansen, and Mattias P. Heinrich. Fast 3d registration with accurate optimisation and little learning for learn2reg 2021. In *Biomedical Image Registration*, *Domain Generalisation and Out-of-Distribution Analysis*, pages 174–179, Cham, 2022. Springer International Publishing. 3
- [48] Hessam Sokooti, Bob de Vos, Floris Berendsen, Boudewijn P. F. Lelieveldt, Ivana Išgum, and Marius Staring. Nonrigid image registration using multi-scale 3d convolutional neural networks. In *Medical Image Computing and Computer As*sisted Intervention - MICCAI 2017, pages 232–239, Cham, 2017. Springer International Publishing. 2
- [49] J.-P. Thirion. Image matching as a diffusion process: an analogy with maxwell's demons. *Medical Image Analysis*, 2(3): 243–260, 1998.
- [50] Laboratory of Neuro Imaging University of Southern California. Loni probabilistic brain atlas (lpba40), 2023. https://loni.usc.edu/research/atlases. 5, 6, 7
- [51] Xiao Yang, Roland Kwitt, Martin Styner, and Marc Niethammer. Quicksilver: Fast predictive image registration a deep learning approach, 2017. 2
- [52] Yungeng Zhang, Yuru Pei, and Hongbin Zha. Learning dual transformer network for diffeomorphic registration. In *Medical Image Computing and Computer Assisted Intervention – MICCAI 2021*, pages 129–138, Cham, 2021. Springer International Publishing. 2
- [53] Zhen Zhao, Sifan Long, Jimin Pi, Jingdong Wang, and Luping Zhou. Instance-specific and model-adaptive supervision for semi-supervised semantic segmentation, 2022. 3
- [54] Jing Zou, Bing Gao, Youyi Song, and Jing Qin. A review of deep learning-based deformable medical image registration. *Frontiers in Oncology*, 12, 2022. 2